Materials Letters 132 (2014) 167–170

Contents lists available at ScienceDirect

Materials Letters

journal homepage: www.elsevier.com/locate/matlet

Fe_3O_4–NiO core–shell composites: Hydrothermal synthesis and toluene sensing properties

Fengdong Qu [a], Yongfan Wang [a], Juan Liu [a], Shanpeng Wen [b,*,1], Yu Chen [c,*,1], Shengping Ruan [a,*,1]

[a] College of Electronic Science and Engineering, Changchun 130012, PR China
[b] State Key Laboratory on Integrated Optoelectronics, Changchun 130012, PR China
[c] Institute of Semiconductors, Chinese Academy of Sciences, Beijing 100083, PR China

ARTICLE INFO

Article history:
Received 10 March 2014
Accepted 9 June 2014
Available online 16 June 2014

Keywords:
Fe_3O_4–NiO
Semiconductors
Sensors
Nanocomposites

ABSTRACT

Fe_3O_4–NiO core–shell composites were prepared via a simple one-step hydrothermal method. The synthesis was conducted in water–ethanol–butanol mixed solvent without any templates. The structure and morphology of the composites were characterized by X-Ray diffraction (XRD), X-Ray photoelectron spectroscopy (XPS) and field emission scanning electron microscopy (FESEM). The results showed that these porous architectures were assembled from Fe_3O_4 sphere core and NiO flower-like shells. To demonstrate the use of the composites, a chemical gas sensor has been fabricated and investigated for toluene detection. The sensor exhibits excellent toluene sensing performances in terms of high response, superior selectivity, and rapid response-recovery.

1. Introduction

Fabrication of nanostructure-based gas sensors which have high sensitivity, selectivity, stability and improved response and recovery time is one of the most significant branches of nanotechnology [1]. Among them, metal oxides, which have a receptor and transducer function, are applied for gas sensing materials as their electrical resistances will change correspondingly upon exposure to oxidizing or reducing gases. It is acknowledged that the gas sensing properties could be influenced by sensing materials' morphologies and structure [2]. Recently, compared to single-metal oxide, hetero-nanostructure composites for gas sensors have attracted great attention because selectivity and response can be manipulated by the component phases [3]. Core–shell nanostructure, one of hetero-nanostructure composites, is an attractive potential material, which is already used as gas sensor and other fields [4–6]. The solution phase route, one of methods to synthesize hetero-nanostructure oxide composites, is considered to be an efficient method for its economical saving, environmental friendly and controllable structure.

Fe_3O_4 and NiO, as two robust semiconductors, have been investigated widely and applied for photocatalysts, gas sensors, and electrodes [7–9]. Many investigations have demonstrated that the performance of two single-metal oxides in gas sensing can be significantly improved by formatting composites [10]. As far as we know, there is few report of synthesizing hierarchical Fe_3O_4–NiO composites.

In this work, we successfully synthesized Fe_3O_4–NiO core–shell composites via the hydrothermal method. The as-prepared products were characterized by various techniques. The XRD pattern and XPS spectroscopy showed that the product had high purity and crystallinity. Furthermore, the FESEM images indicated that these porous architectures were assembled from Fe_3O_4 sphere core and NiO flower-like shells. When evaluated as the sensing material for gas sensor, the as-prepared Fe_3O_4–NiO core–shell composites manifested balanced characteristics to toluene.

2. Experimental section

$FeSO_4 \cdot 7H_2O$, urea, trisodium citrate, butanol and ethanol were purchased from Beijing Chemicals Co., Ltd. (Beijing, China). $NiCl_2 \cdot 6H_2O$ was purchased from Xilong Chemical Reagent Co. (Guangdong, China). All of these chemicals were analytical grade and used without any further purification. In a typical process, $FeSO_4 \cdot 7H_2O$ (0.14 g, 0.5 mmol) was dissolved in a mixture of water (20 ml), ethanol (12 ml) and butanol (1 ml) to form a clear solution, followed by the addition of $NiCl_2 \cdot 6H_2O$ (0.34 g, 1.25 mmol), trisodium citrate (Na_3Cit) (0.10 g) and urea (0.16 g).

* Corresponding authors.
E-mail addresses: sp_wen@jlu.edu.cn (S. Wen), chenyu_1099@163.com (Y. Chen), ruansp@jlu.edu.cn (S. Ruan).
[1] Tel./fax: +86 431 85168242.

http://dx.doi.org/10.1016/j.matlet.2014.06.060
0167-577X/

The mixture was stirred vigorously for 30 min and then transferred to a Teflon-lined stainless-steel autoclave (50 ml capacity). The autoclave was heated and maintained at 120 °C for 5 h, and then cooled to room temperature. The resulting green precursor was washed several times and dried in vacuum at 60 °C for 4 h. Then, the obtained powders were calcined in air at 300 °C for 2 h, and Fe_3O_4–NiO core–shell composites were prepared.

X-Ray diffraction (XRD) analysis was conducted on a Scintag XDS-2000 X-ray diffractometer with Cu Kα radiation ($\lambda = 1.5418$ Å). X-Ray photoelectron spectroscopy (XPS) data was obtained with a VG ESCALAB MK II spectrometer with an Mg KR excitation (1253.6 eV). Field emission scanning electron microscopy (FESEM) images were performed on a SHIMADZU SSX-550 (Japan) instrument.

The details of the sensor fabrication were similar to our previous work [11]. Gas sensing properties were measured by CGS-8 intelligent gas sensing analysis system (Beijing Elite Tech Co., Ltd., Beijing, China) under laboratory condition (25 °C, 40 RH%).

3. Results and discussion

A typically powder XRD pattern of the product is shown in Fig. 1a. It reveals that the products consist of two substances. The diffraction peaks in the XRD pattern are in good agreement with Fe_3O_4 (JCPDS card: 75-0049) and NiO (JCPDS card: 78-0429). No other diffraction peaks corresponding to impurities were observed, which implied the purity of Fe_3O_4 and NiO crystal formation. Besides, surface analysis of the as-synthesized flower like Fe_3O_4–NiO core–shell composites was carried out by XPS. The XPS spectra in different spectral regions, which are shown in Fig. 1b, display the binding energies for Ni 2p, Fe 2p, O 1s and C 1s of the samples. The binding energy for C 1s peak (284.0 eV) was used as an internal reference [12]. It can be seen that the intensity of Ni peaks is higher than that of Fe peaks, which possibly confirms that the hierarchical microspheres have a core–shell structure. Fig. 1c shows two intense bands (725.4 eV and 712.7 eV) those are assigned to Fe $2p_{1/2}$ and Fe $2p_{3/2}$, respectively. Both these bands consist of Fe^{2+} and Fe^{3+} peaks and are typical characteristics of Fe_3O_4 structure [13]. The Ni 2p XPS spectrum (Fig. 1d) shows two edges of Ni $2p_{1/2}$ and Ni $2p_{3/2}$, which confirms the presence of the corresponding elements for NiO shell [14]. The Ni $2p_{1/2}$ main peak and its satellite (872.6 eV and 879.8 eV), and Ni $2p_{3/2}$ main peak and its satellite (853.9 eV and 861.1 eV) were assigned to the Ni^{2+} in NiO. The shoulder peak at 855.0 eV may be attributed to the Ni^{2+} species on the surface [15]. The energy difference between Ni $2p_{3/2}$ and Ni $2p_{1/2}$ splitting was 15.3 eV, which indicated the well-defined symmetry of Ni^{2+} in oxide form.

Fig. 2 shows the FESEM images and EDX spectra of the obtained Fe_3O_4–NiO core–shell composites, elucidating their morphologies and microstructural features. Fig. 2a and b shows the low- and high-magnification FESEM images of Fe_3O_4–NiO core–shell composites, respectively. According to the images, the flower-like microspheres have a diameter of about 700 nm. Fig. 2c gives out the high-magnification SEM image of the NiO shell. Fig. 2d gives out the FESEM image of a broken Fe_3O_4–NiO microsphere, from which we can observe the core–shell structure. EDXS confirms the core–shell composites are composed of Fe, Ni and O elements (Fig. 2e). The Si in the spectra was assigned to the SEM grid used to support the sample.

In order to reveal the formation process of the core–shell composites, morphology evolution of the composites was investigated in detail as a function of reaction time, which is shown in Fig. 3. It can be found that there was rarely shaped product in 2 h (Fig. 3a). When the time reached 3 h, there appeared Fe_3O_4 microspheres. When the time was further increased to 4 h, the

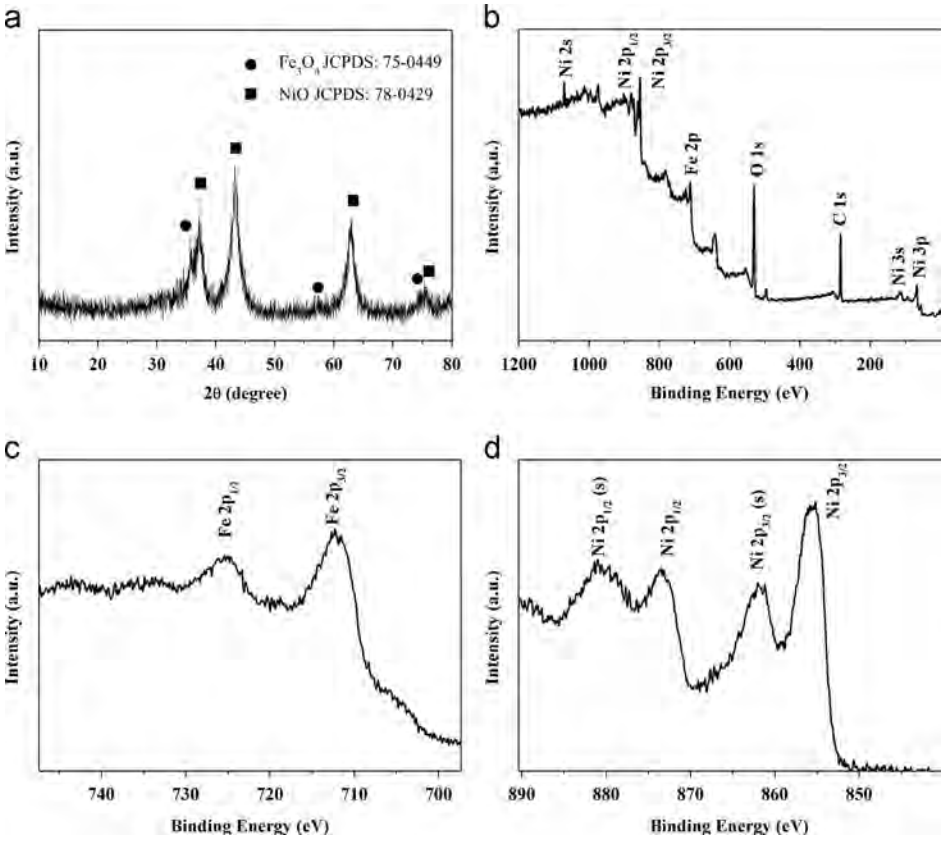

Fig. 1. XRD pattern (a), and XPS spectra (b) full spectrum; (c) Fe 2p; (d) Ni 2p of Fe_3O_4–NiO core–shell composites obtained at the reaction time of 5 h.

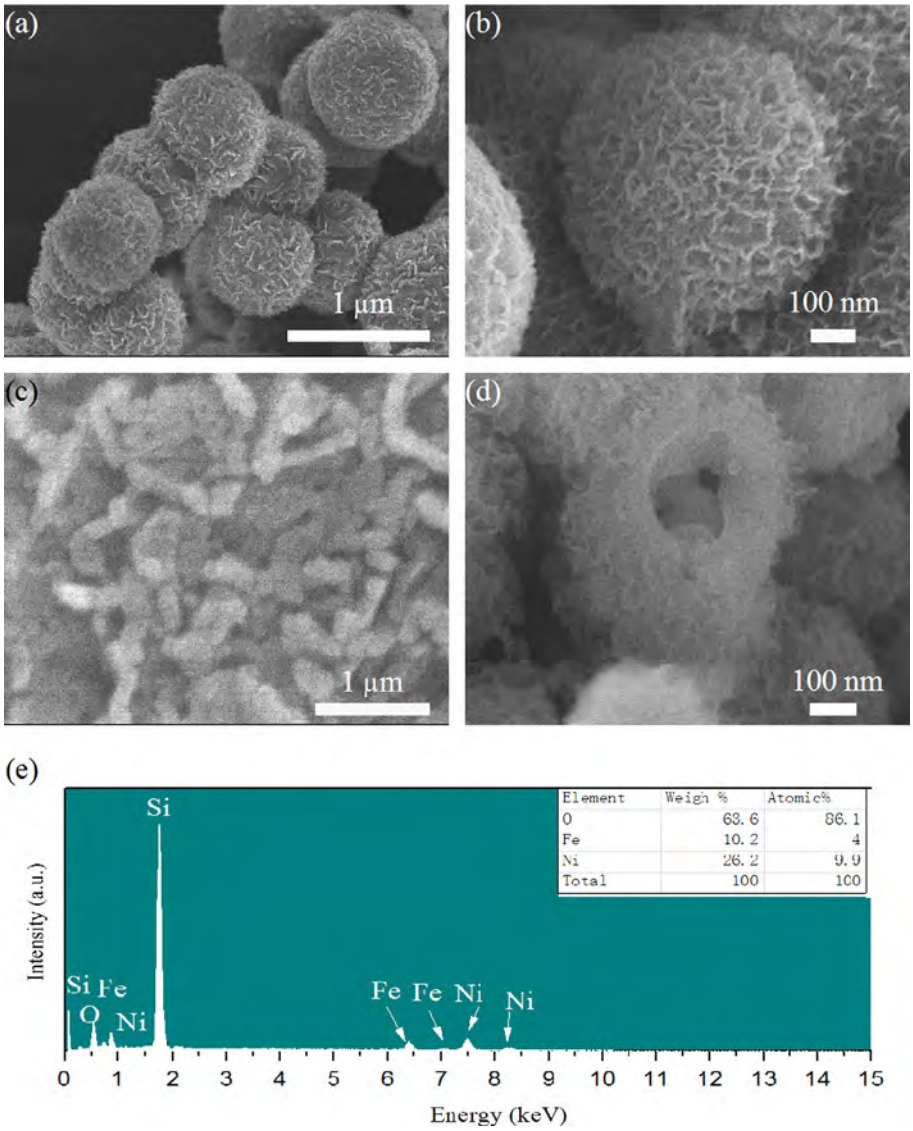

Fig. 2. (a–d) FESEM images, (e) EDX spectra of the Fe_3O_4–NiO core–shell composites obtained at the reaction time of 5 h.

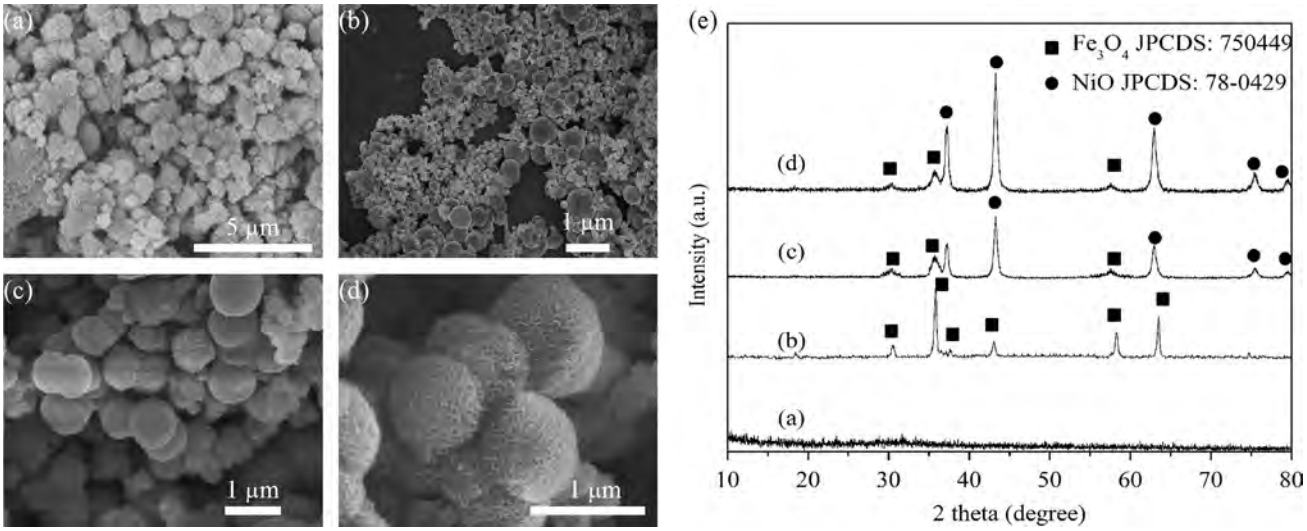

Fig. 3. (a–d) FESEM images and (e) XRD patterns of the products obtained at the reaction time of (a) 2 h, (b) 3 h, (c) 4 h and (d) 5 h.

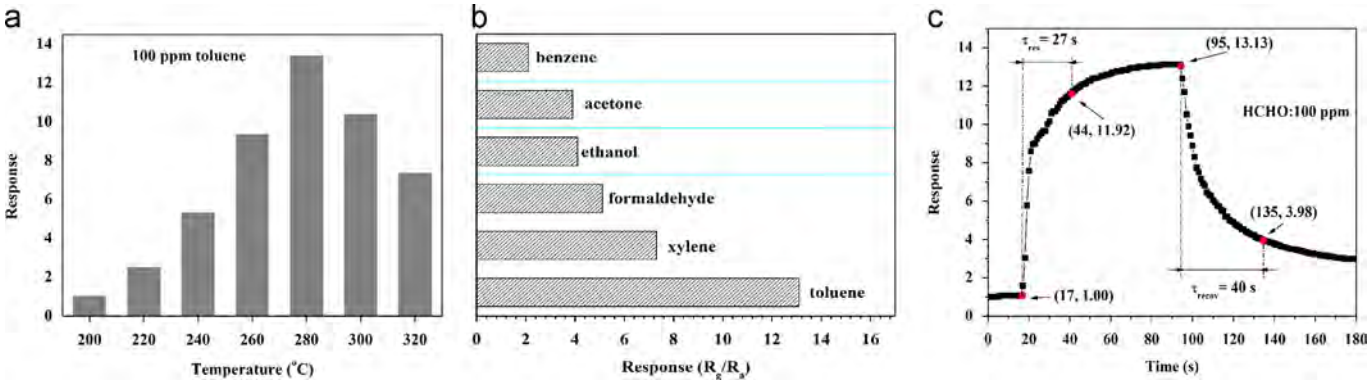

Fig. 4. (a) Response of sensor based on the as-prepared core–shell nanoarchitecture to 100 ppm toulene as a function of the operating temperature; (b) response of sensor based on hierarchical Fe_3O_4–NiO core–shell nanostructure to 100 ppm various gases at 280 °C; (c) The dynamic response–recovery curves of the sensor to 100 ppm toluene at 280 °C.

cores all grew well and some shells appeared which was shown in Fig. 3c. With a further increase to 5 h, the core–shell structure had already formed (Fig. 3d). In order to prove the components of the products obtained above, the XRD patterns of the products were measured and shown in Fig. 3e.

It is acknowledged that the response of a semiconductor gas sensor is highly influenced by the operating temperature [16]. The responses of the sensor based on Fe_3O_4–NiO core–shell microspheres to 100 ppm toluene were tested as function of operating temperature to determine the optimum temperature, which is shown in Fig. 4a. It is apparent that the response of the sensor varied with different operating temperature. The response to toluene rapidly increased and reached the maximum at the operating temperature of 280 °C, and then decreased with a further increase of the operating temperature.

The selectivity of the sensor based on Fe_3O_4–NiO core–shell microspheres was measured on exposure to different volatile organic compounds (VOCs) (100 ppm) at the operating temperature of 280 °C, which is shown in Fig. 4b. The result showed that the sensor had an obvious response to toluene, and less effective response to other tested gases. Response and recovery times are important factors of gas sensors: fast response and recovery can usually allow a real-time detection. Fig. 4c showed the dynamic response–recovery curves of the sensor to 100 ppm toluene at 280 °C. The τ_{res} and τ_{recov} of the sensor are 27 and 40 s, respectively.

4. Conclusions

In summary, we reported the synthesis of Fe_3O_4–NiO core–shell microspheres via the facile hydrothermal method free of any templates. The images of field emission scanning electron microscopy indicated that these porous architectures were assembled from Fe_3O_4 sphere core and NiO flower-like shells. When applied for sensing materials in gas sensor, the excellent toluene sensing properties were observed, which indicate that the sensor based as-prepared composites is a potential candidate for high performance toluene gas sensors.

Acknowledgments

This work was supported by the National Natural Science Foundation of China (Grant nos. 61077046, 61274068, and 61275035), Chinese National Programs for High Technology Research and Development (Grant no. 2013AA030902), Project of Science and Technology Development Plan of Jilin Province (Grant nos. 20110314, and 20120324), and the Opened Fund of the State Key Laboratory on Integrated Optoelectronics (No. IOSKL2012KF03).

References

[1] Franke ME, Koplin TJ, Simon U. Small 2006;2:36–50.
[2] Gurlo A. Nanoscale 2011;3:154–65.
[3] Lee J-H. Sens Actuators B 2009;140:319–36.
[4] Jiang Z, Xue S, Wu S, Zou R, Zhang Z, Jang M. Mater Lett 2013;105:239–41.
[5] Ye M, Zhang Q, Hu Y, Ge J, Lu Z, He L, et al. Chem-Eur J 2010;16:6243–50.
[6] Liu J, Jiang J, Cheng C, Li H, Zhang J, Gong H, et al. Adv Mater 2011;23:2076–81.
[7] Wen Z, Tian-mo L. Physica B 2010;405:1345–8.
[8] Xuan S, Jiang W, Gong X, Hu Y, Chen Z. J Phys Chem C 2009;113:553–8.
[9] Shifu C, Sujuan Z, Wei L, Wei Z. J Hazard Mater 2008;155:320–6.
[10] Guo W, Liu T, Sun R, Chen Y, Zeng Y, Wang Z. Mater Lett 2012;89:5–8.
[11] Liu J, Guo W, Qu F, Feng C, Li C, Zhu L, et al. Ceram Int 2014;40:6685–9.
[12] Hu J, Zhu K, Chen L, Yang H, Li Z, Suchopar A, et al. Adv Mater 2008;20:267–71.
[13] Lo CK, Xiao D, Choi MMF. J Mater Chem 2007;17:2418–27.
[14] Peck MA, Langell MA. Chem Mater 2012;24:4483–90.
[15] Tomellini M. J Electorn Spectrosc 1992;58:75–8.
[16] Shinde VR. Sens Actuators B 2007;123:701–6.